Applied Thermal Engineering 243 (2024) 122635

Contents lists available at ScienceDirect

Applied Thermal Engineering

journal homepage: www.elsevier.com/locate/apthermeng

Research Paper

The effect of driving voltage waveforms on the efficiency of linear compressor

Nibin Qian [a], Chunhui Yang [a], Changtong Xu [a], Zhaohua Li [b], Kun Liang [a,*], Zhennan Zhu [c], Xinwen Chen [d]

[a] Department of Engineering and Design, University of Sussex, Brighton BN1 9QT, UK
[b] College of Mechanical Engineering, Yangzhou University, Yangzhou 225012, China
[c] Department of Chemical Engineering, Imperial College London, London SW7 2AZ, UK
[d] School of Automotive Engineering, Tongji University, Shanghai 201804, China

ARTICLE INFO

Keywords:
Linear compressor
Voltage waveform
Stroke control
Body pressure
Adiabatic efficiency
Piston motion

ABSTRACT

Linear compressors, known for their oil-free operation and elimination of crank mechanism, have found extensive applications in cryocoolers and domestic refrigeration. The efficiency improvement of linear compressor is crucial for refrigerators and cryocoolers, particularly in space application. This paper experimentally studies the impact of driving voltage waveforms on the efficiency of linear compressors, employing four different waveforms for comprehensive analysis: sine wave without crest, sine wave without trough, sine wave, and sine wave without both crest and trough. By fixing compressor stroke and piston offset, the results show that the sine wave without a crest and sine wave without a trough outperform the sine wave and sine wave without both crest and trough in terms of mass flow rate and adiabatic efficiency. The sine wave without a trough demonstrates an 8% enhancement in adiabatic efficiency compared to the standard sine wave. This superior performance is attributed to the reduction in body pressure variation because of faster arrival at datum position, causing lower gas leakage across the radial clearance gap.

1. Introduction

In recent years, high-efficiency cryocoolers have been urgently needed in many fields such as superconducting and quantum computing, to satisfy the cooling requirements, for which linear compressors have emerged as an ideal choice in cryocoolers [1]. Most recently, linear compressor has been extended to domestic refrigeration [2,3,4], capable of lower power consumption and higher seasonal performance [5]. A linear compressor is directly driven by a linear motor and eliminates crank mechanism. It has potential to achieve oil-free operation [6]. Because of these characteristics, linear compressors offer numerous advantages, such as a broad selection of working fluids, low friction, extended operational life, high efficiency, and compact structure [7]. The stroke of a linear compressor is adjustable, allowing it to meet various cooling capacity demands while operating at its resonant frequency for maximum efficiency [8,9,10,11]. Liang et al. [12] pointed out that the overall efficiency of linear compressor can be 33 % higher than traditional reciprocating compressors.

The field of linear compressors has seen development over the years by various companies and researchers. The Oxford-type linear compressor [13] is one of the most typical linear compressors. The former three generations are driven by moving coil motor [14], and Liang et al. [6] updated it with moving magnet linear motor which enhanced force capacity and energy efficiency. The Oxford-type compressor uses spiral flexure springs for piston support and employs a non-contacting clearance seal without oil to ensure low-friction operation. Sunpower company developed moving magnet linear compressor with a gas bearing system [15] for CPU cooling. This motor features a tubular magnet, and its coil, circumferentially wound, is housed within the outer pole assembly's laminations, facilitating high motor efficiency. However, the incorporation of the tubular magnet does introduce complexity in assembly. In 2000, LG electronics company licensed Sunpower linear compressor for domestic refrigerator [16], which is 20–30 % more efficient than crank drive compressor. Lee et al. [17] presented a linear compressor for air conditioner. Due to the 1000–6000 W high load of air conditioner, the required coil springs assembly is very large, which makes the linear compressor bulky and heavy (14 kg).

A number of studies have been conducted on improving the

* Corresponding author at: Department of Engineering and Design, University of Sussex, Brighton BN1 9QT, UK.
E-mail address: kun.liang@sussex.ac.uk (K. Liang).

https://doi.org/10.1016/j.applthermaleng.2024.122635
Received 2 December 2023; Received in revised form 23 January 2024; Accepted 1 February 2024
Available online 7 February 2024

Nomenclature

Abbreviation

a	amplitude (mm) and piston offset (mm)
BEMF	back electromotive force (V)
COP	coefficient of performance
DAQ	data acquisition
LDAQ	low-speed data acquisition
LVDT	linear variable differential transducers
$\dot{m}$	mass flow rate (g/s)
n	harmonic term and adiabatic index
P	power (W) and pressure (bar)
PID	proportional-integral-derivative
R	specific gas constant
S	stroke
T	temperature (°C)
TDC	top dead centre

Greek symbol

η	efficiency

Subscripts

dis	discharge
g	gas
i	input
suc	suction
a	adiabatic

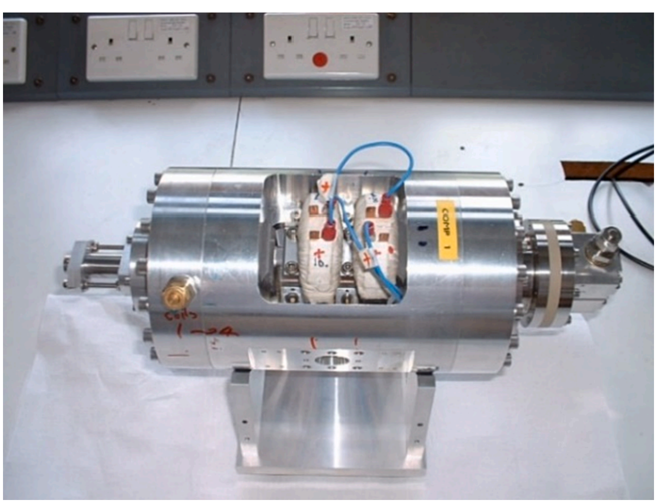

Fig. 1. Prototype of novel oil-free moving magnet linear compressor.

Table 1
Parameters of linear compressor [26].

Total mass of piston (kg)	0.66
Resistance of coil (Ω)	3.5
Mechanical spring rate (N/mm)	17
The distance between the datum position and cylinder head (mm)	7.57
Piston diameter (mm)	18.99
Piston length (mm)	31
Maximum stroke (mm)	14
Radial clearance (μm)	10
Operating frequency (Hz)	30–50
Capacitor (μF)	150
Inductance (H)	0.141

performance of linear compressors. Liang et al. [18] added a bleed cycle in linear compressor to counteract piston offset and increase volume efficiency. You et al. [19] pointed out that the in phase of current and velocity can achieve the highest input power. Jiang et al. [20] found that the smaller clearance volume can decrease the motor efficiency but increase COP (coefficient of performance). Zhu et al. [21] developed a resonance frequency track method that can find resonance frequency with a phase monitor. Besides, Optimisation of waveforms for driving voltage and piston motion has drawn attention from several researchers: Tang and Dang [22] compared the effects of three driving voltage waveforms (sine wave, trapezoid wave, and smeared sine wave) in a Stirling pulse tube cryocooler powered by a dual-opposed moving coil linear compressor. The trapezoid wave and smeared sine wave respectively show 6.8 % and 9.6 % higher COP than sine wave. This is due to the non-sine waveforms leading to a reduced phase difference between dynamic pressure and volume flow rate, which influences cooling capacity. Additionally, the effective value of the current is reduced, resulting in decreased coil losses that are proportional to the square of the current. However, these two waves introduce increased compressor vibrations when input power exceeds 60 W, which can reduce the cooling performance; Li et al. [23] examined the influences of sine wave, square wave, sine wave without trough, and sine wave without both crest and trough. Their findings showed that the sine wave demonstrated superior motor efficiency for linear compressor compared to other waves. But the COP of the sine wave without the trough surpassed the sine wave by 11 % at 60 Hz. This was ascribed to the difference of electromagnetic forces caused by the single side clipped sine wave, which counteract a part of piston offset. It is evident that the single side clipping of driving voltage waveform benefits the performance of linear compressor. However, this study lacked a comparison between different side clipped waveforms; Wei et al. [24] assessed the influence of five different displacement profiles using a numerical model of a dual piston linear compressor powered by a three-phase permanent magnet

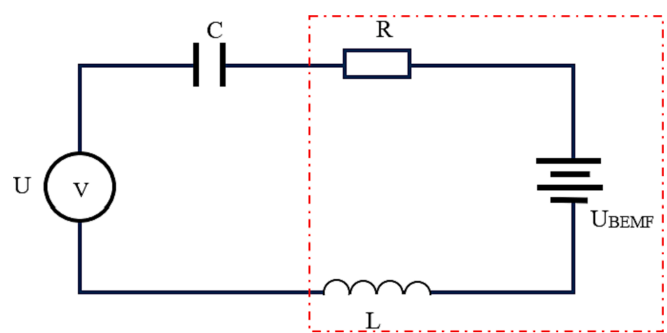

Fig. 2. RLC circuit for the linear motor.

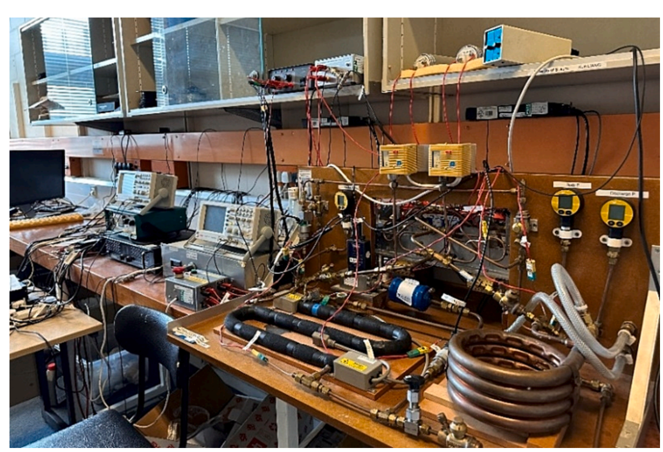

Fig. 3. Test rig for the linear compressor waveform experiments.

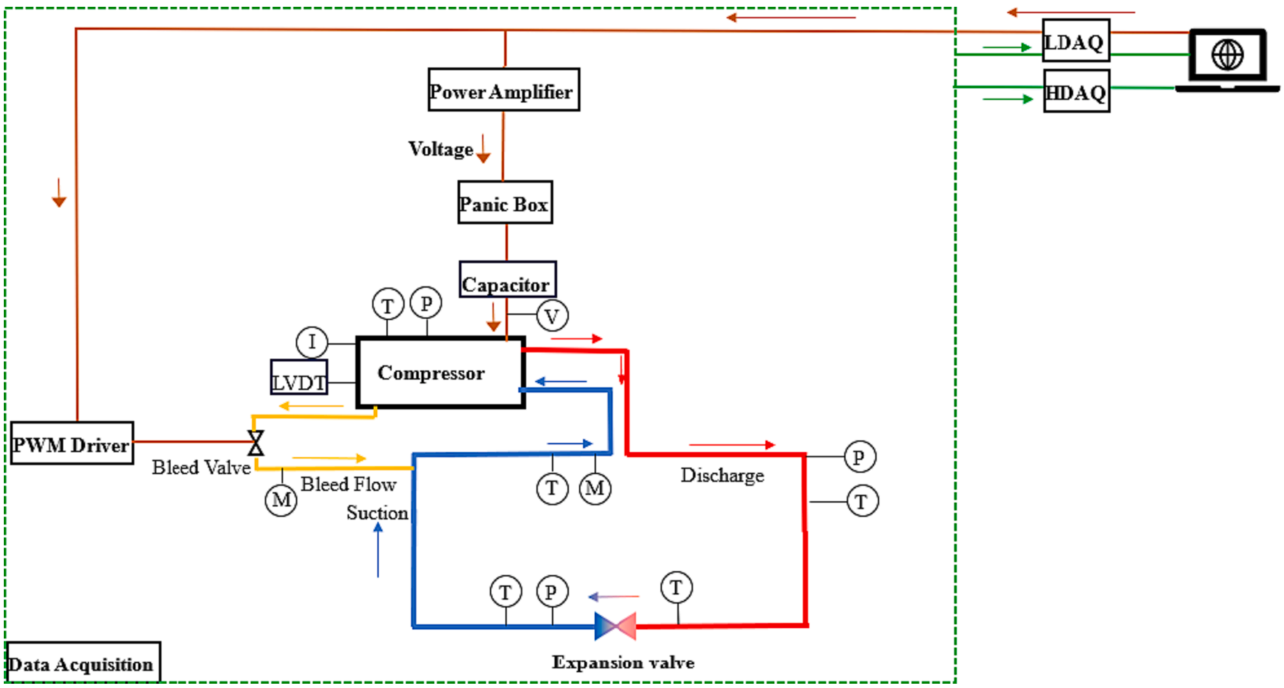

Fig. 4. Schematic of linear compressor test rig (T: temperature transducer; P: pressure transducer; V: voltage sensor; I: current transducer; LVDT: displacement transducer; M: mass flow meter; blue and red lines: main loop; yellow line: bleed loop). (For interpretation of the references to colour in this figure legend, the reader is referred to the web version of this article.)

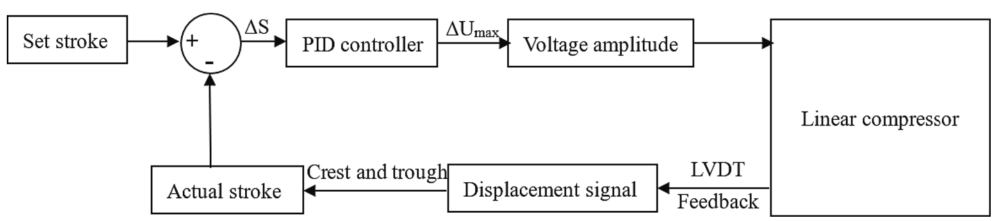

Fig. 5. Schematic of the PID controller for the linear compressor stroke.

Table 2
Specifications and accuracies of the instruments for the test rig.

Instruments	Model	Quantity	Accuracy (refer to value)
Pressure transducer	DRUCK PMP1400	4	±0.15 %
Current transducer	LA LEM 25-NP	1	± 0.5 %
Voltage attenuator	Fylde 261HVA HV	1	±0.5 %
LVDT	Lucas Schaevitz	1	±0.025 mm
LVDT signal conditioner	ATA-101	1	N/A
Main mass flow meter	Hastings HFM-201	1	±1 %
Bleed flow meter	Tylan FM-360	1	±1 %
Isolation amplifier	Fylde 4600A	1	±0.5 %
AC power amplifier	Vonyx VXA-2000(class A)	1	±1.2 dB
Oscilloscope	RS Pro IDS1000Series IDS1072AU	3	N/A
Data acquisition card	NI USB-6341	2	N/A

synchronous motor, concluding that the triangle curve (case 3) performs better. This is attributed to the shorter expansion process resulting from the triangle curve, which leads to longer suction process, thereby enhancing compression efficiency. Additionally, the triangle curve produces a lower peak piston velocity, resulting in smaller back electromotive force (BEMF), which improved motor efficiency; Silva and Dutra [25] established a numerical model of a reciprocating compressor incorporating a genetic optimisation algorithm to find the optimum piston trajectory at specific operating conditions. They divided the piston trajectory to four velocity stages, which time and velocity value constraints were added for each stage that can achieve maximum

Table 3
Experiment conditions for the linear compressor waveforms.

Fluid	Nitrogen
Pressure ratio	2, 2.5, 3, 3.5
Stroke (mm)	8, 10, 12
Operating frequency (Hz)	Resonant frequency
Driving voltage waveform	Sine wave Sine wave without crest Sine wave without troughsine wave without crest and trough

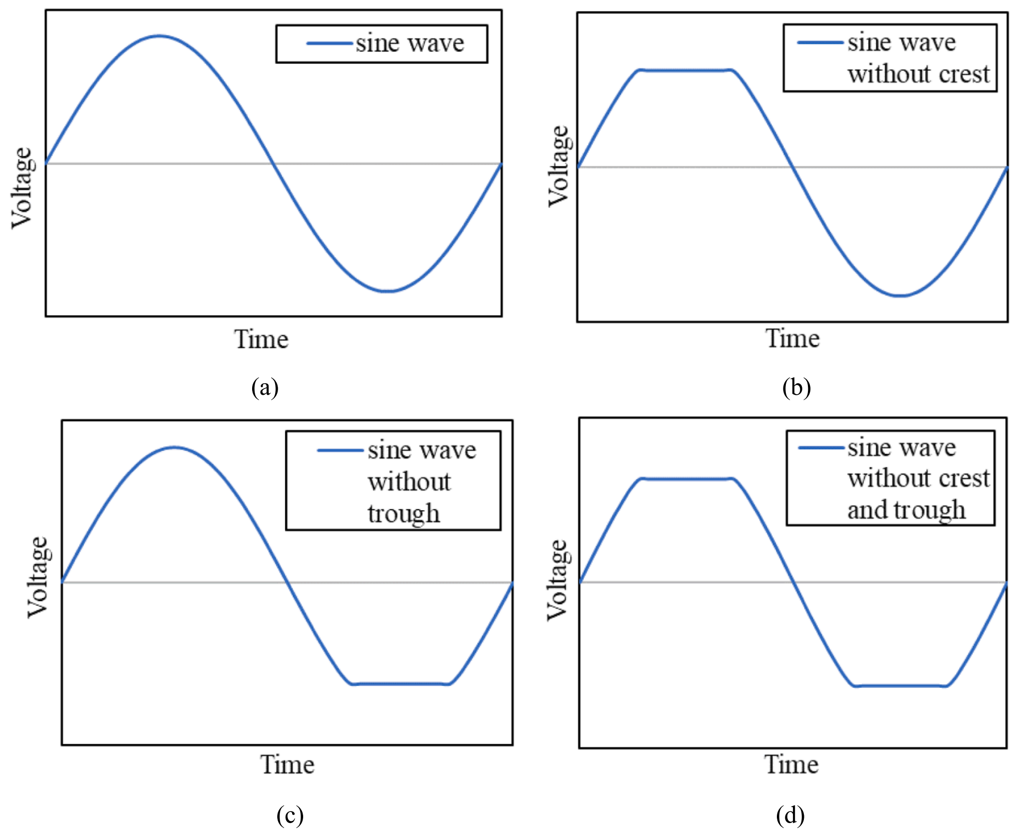

Fig. 6. Four types of driving voltage waveforms (a) sine wave. (b) sine wave without crest. (c) sine wave without trough. (d) sine wave without crest and trough.

thermodynamic efficiency. Then the optimum piston trajectory will be found through optimisation process. Compared with a crank-rod compressor, the optimum piston trajectory can increase thermodynamic efficiency by 25.6 % when the evaporator temperature is −35 ℃ and the condenser temperature is 65 ℃. However, this approach is only viable with static boundary conditions.

Despite 4 studies mentioned above that investigated waveform effects, the mechanism has not been fully understood. Besides, in practical case, the compressor stroke and piston offset will need to be fixed when comparing different waveforms which were not implemented in any literature studies. The present study experimentally investigated the effects of four different driving voltage waveforms on the performance of a linear compressor at different strokes and pressure ratios by keeping stroke constant and piston offset at zero. These four waveforms included: sine wave, sine wave without crest, sine wave without trough, and sine wave without both crest and trough.

2. Linear compressor and test rig

2.1. Linear compressor

The oil-free moving magnet valved linear compressor for experiments is shown in Fig. 1 which was developed by Liang [26] for both Joule-Tompson cryocooler and domestic refrigerator. The compressor is composed of several key components: a free magnet-piston assembly, a suspension system with flexure springs, a pair of reed valves and a moving magnet linear motor. Table 1 shows the specific parameters for the prototype linear compressor.

A 100 W moving magnet linear motor was developed. The piston linear motion is ensured by two axially separated flexure springs. Two reed valves located on the cylinder head are for suction and discharge respectively. The equivalent electric circuit of the linear motor is shown in Fig. 2. A capacitor was adopted to reduce the voltage input whilst ensuring resonant operation of the linear compressor. ‘U’ is the input driving voltage, and the compressor voltage is the sum of resistance, BEMF and inductance voltages in red frame, which is measured in the test rig (Section 2.2). In this work, the waveform of the driving voltage was adjusted to study the effect on the compressor efficiency.

2.2. Test rig for experiment

To assess the performance of a linear compressor driven by different voltage waveforms, the linear compressor was instrumented in a test rig as shown in Fig. 3 using nitrogen as working fluid and Fig. 4 shows the schematic of the test rig. The pressure ratio of the test rig is controlled by adjusting expansion valve. The compressor draws in low-pressure working fluid from suction valve and compresses it, converting it into high-pressure gas. The fluid then flows out of the compressor through the discharge valve, traveling to the expansion valve where the pressure is released. Finally, the fluid flows back into the suction valve.

A PID (proportional-integral-derivative) control system for the compressor stroke as Fig. 5 shows was incorporated in the test rig to keep stroke constant when adjusting the voltage waveforms. A LabVIEW based PID controller in the computer generates an analogue signal for the voltage amplitude, then pass through the LDAQ (low-speed data acquisition) card to the AC amplifier to amplify the signal and drive the linear compressor. Actual stroke is determined based on the displacement measured by the LVDT, and it is compared with the set stroke to calculate the stroke error. The PID controller adjusts the voltage amplitude in response of stroke error (ΔS) to eliminate the error.

During compressor operation, the gas leakage across the radial clearance gap between the compression chamber and body side can lead to drift of datum position that the piston oscillates about, which is also named as piston offset in literature. The presence of piston offset will reduce the effective stroke and consequently affect compressor performance. In this work, a bleed loop was employed to eliminate the piston offset by recirculating the gas leakage from compressor body back to suction port. The PID controller modulates the duty cycle of the solenoid valve to regulate the bleed flow keeping the piston offset at zero for all operating conditions and voltage waveforms during testing.

2.3. Instruments

The instruments on test rig are listed in Table 2. Four DRUCK PMP1400 are for pressure measuring. A LA LEM 25-NP and a Fylde 261HVA HV are used for current transducer and voltage attenuator respectively. The displacement of linear compressor is monitored by a Lucas Schaevitz LVDT. A mass flow meter (Hastings HFM-201) is for main flow measurement in the refrigerant loop and another meter (Tylan FM-360) is used to measure the bleed flow. Besides, two oscilloscopes were employed to observe the real time current, voltage, and displacements of the linear compressors. An alternating current (AC) power amplifier is required to enlarge the driving voltage signal to satisfy linear compressors operation due to the maximum output voltage of DAQ card is 5 V.

3. Experiment conditions

The experimental conditions are listed in Table 3. The frequency was manually adjusted to resonant frequency to allow resonant operations.

Four driving voltage waveforms as shown in Fig. 6 were tested, including sine wave, sine wave without crest, sine wave without trough, and sine wave without both crest and trough. The sine wave without crest and sine wave without trough are single side clipped sine waves. The results from the sine wave are used as a benchmark against other three waveforms. The waveform was automatically modulated in LabVIEW. For the three non-sine waveforms, an original sine wave voltage was generated by PID controller and then the maximum/minimum values were truncated at 75 %.

4. Results and discussions

4.1. Mass flow rate

Fig. 7 shows the mass flow rate and specific mass flow rate against stroke for four different driving voltage waveforms at a pressure ratio of 3. As the stroke increases, mass flow rate rises linearly for all voltage

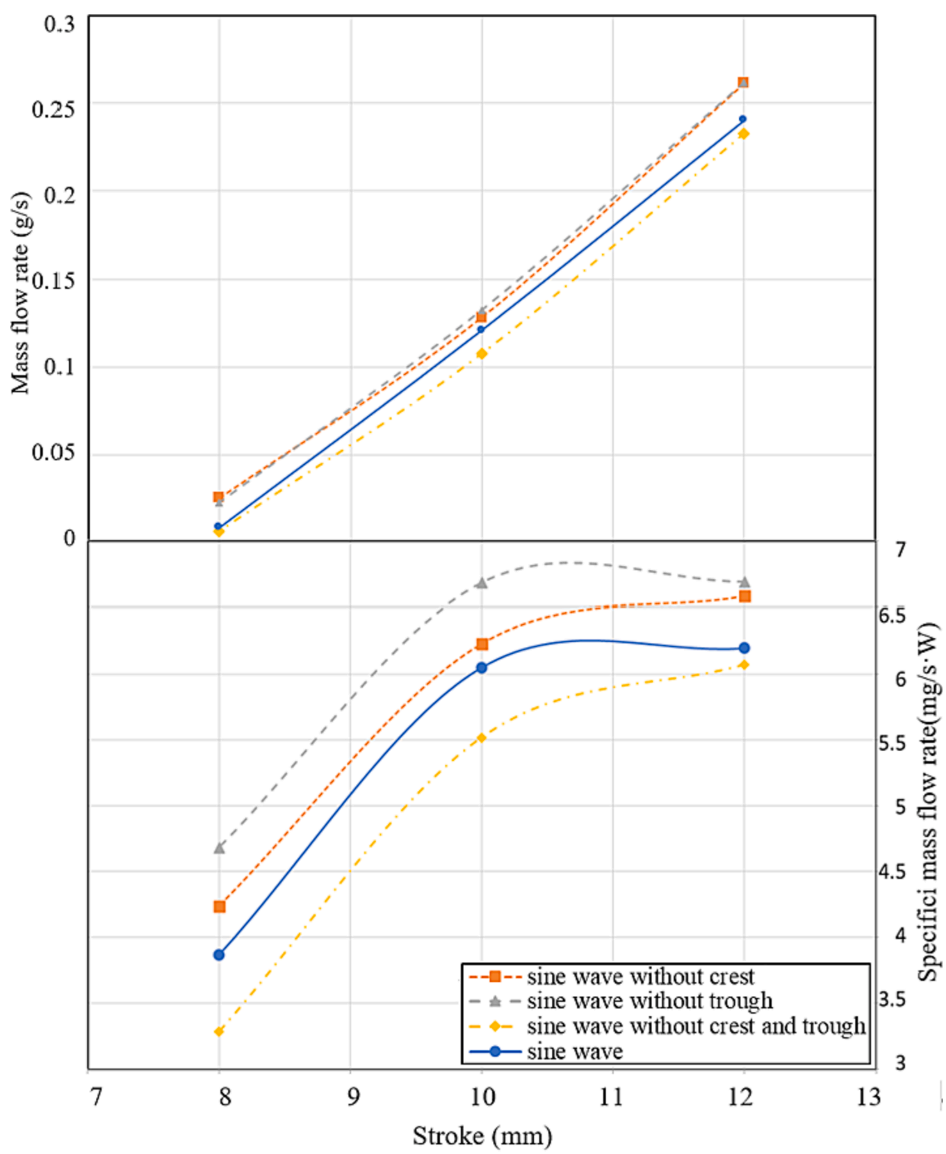

Fig. 7. Mass flow rate and specific mass flow rate against stroke for four different driving voltage waveforms with pressure ratio of 3.

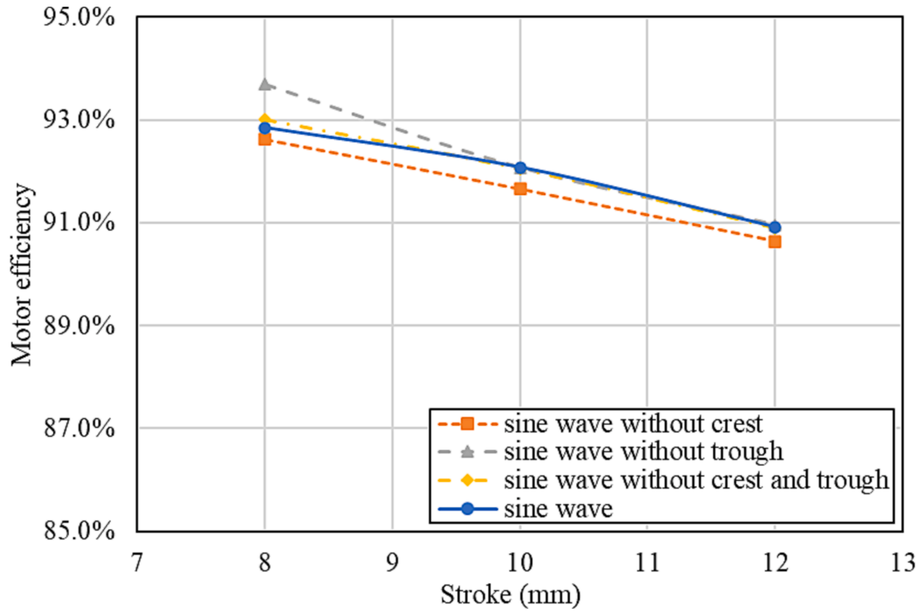

Fig. 8. Motor efficiency against stroke for four different driving voltage waveforms with pressure ratio of 3 and frequency of 31 Hz.

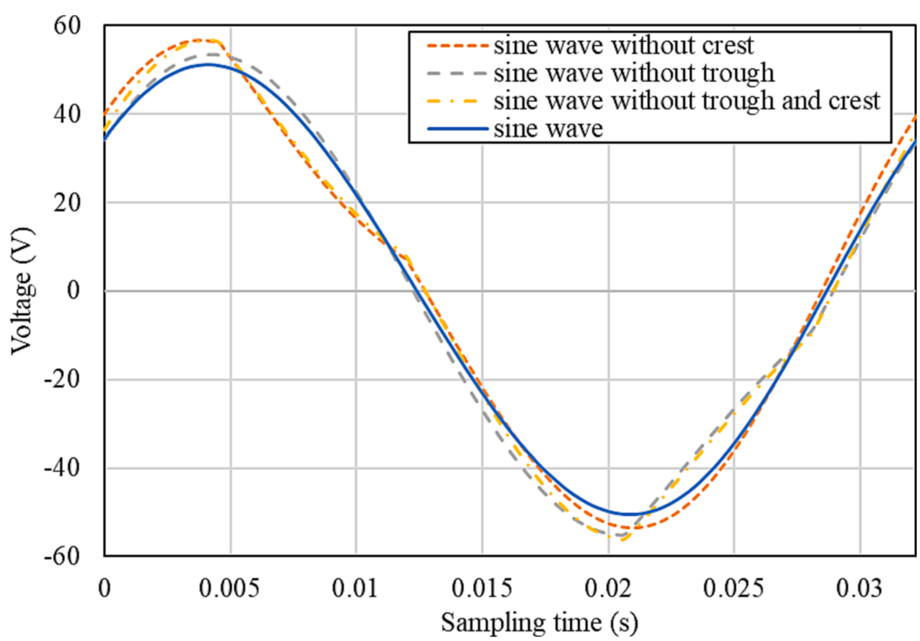

Fig. 9. Linear compressor voltage for four different driving voltage waveforms with stroke of 12mm, pressure ratio of 3 and frequency of 31 Hz.

waveforms. The mass flow rates are close for sine wave without crest and sine wave without trough, which is nearly 8 % higher than sine wave at stroke of 12 mm. The specific mass flow rate which is mass flow rate divided by input power. The sine wave without a trough has the highest specific mass flow rate, that is 10.4 % higher than the sine wave at stroke of 10 mm. But the specific mass flow rate difference between two single side clipped waveforms decreases as the stroke increases to 12 mm.

4.2. Motor efficiency

Fig. 8 shows the motor efficiency in relation to strokes for four different driving voltage waveforms with a pressure ratio of 3. The motor efficiency decreases linearly with increased stroke. Four efficiency curves are very close to each other with only 1 % maximum difference.

Because of the stroke PID control, for the modulated waveform, the input voltage on the clipped side was elevated to allow the piston to reach the preset stroke. This increase results in deformation of the linear compressor voltage, as shown in Fig. 9.

4.3. Adiabatic efficiency

The adiabatic power [27] can be determined as

$$P_a = \frac{n}{n-1}\dot{m}R_g T_{suc}[\left(\frac{P_{dis}}{P_{suc}}\right)^{\frac{n-1}{n}} - 1] \tag{1}$$

where n is the adiabatic index, $\dot{m}$ is the mass flow rate, R_g is the specific gas constant, T_{suc} is the suction temperature, P_{dis} and P_{suc} are the discharge pressure and suction pressure of cylinder respectively.

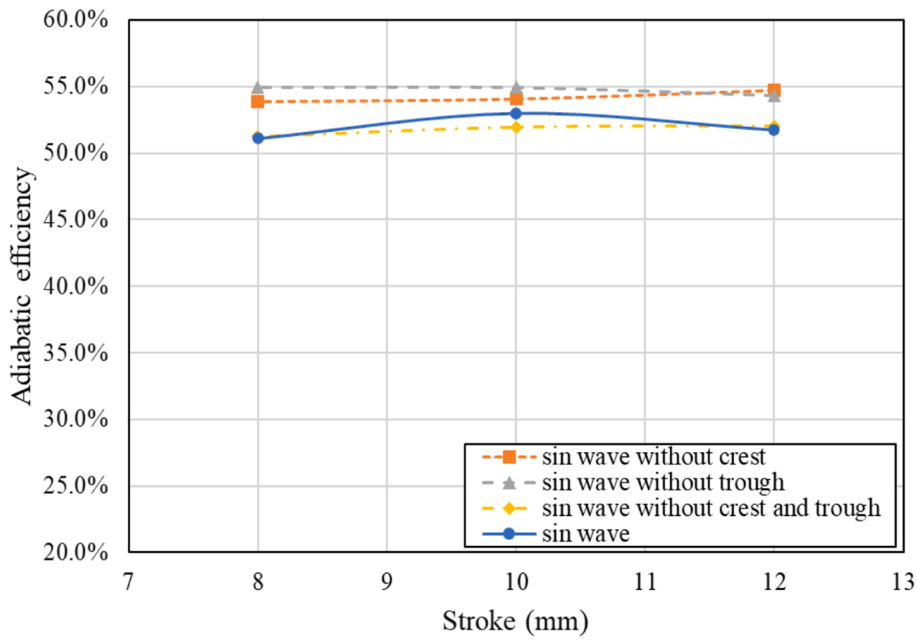

(a)

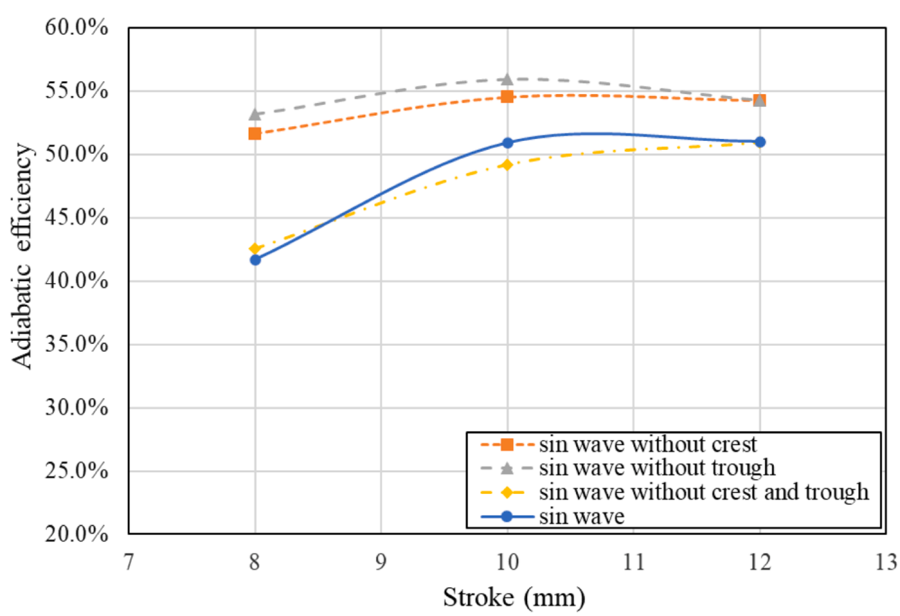

(b)

Fig. 10. Adiabatic efficiency against stroke for four different driving voltage waveforms: (a) pressure ratio of 2; (b) pressure ratio of 2.5; (c) pressure ratio of 3.

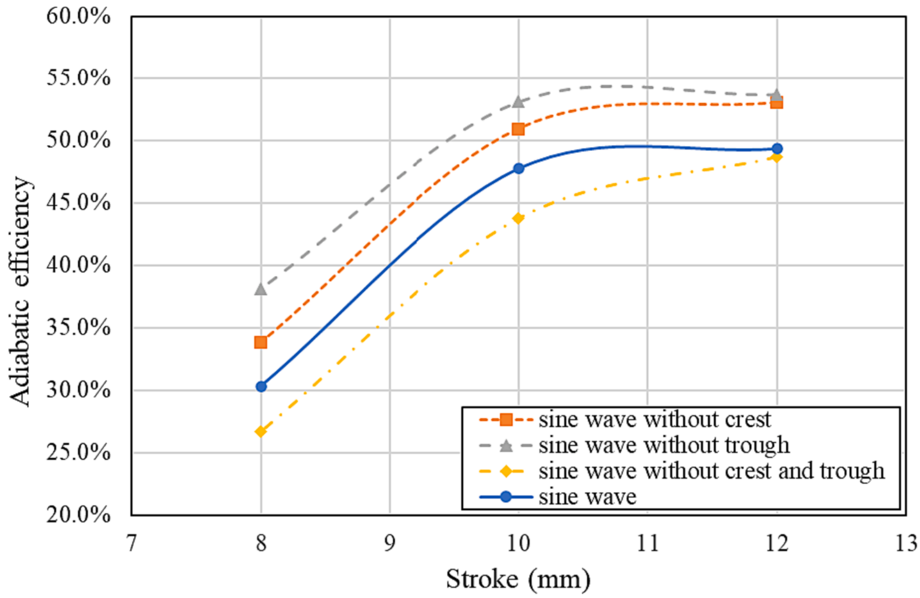

(c)

Fig. 10. (*continued*).

Thus, the adiabatic efficiency is

$$\eta_a = \frac{P_a}{P_{in}} \tag{2}$$

where P_{in} is the input power.

Fig. 10 plots the adiabatic efficiency against stroke for various pressure ratios and driving voltage waveforms. As the pressure ratio moves from 2 to 3, differences among waveforms increase: At a pressure ratio of 2, the adiabatic efficiency curves for four waveforms are very close to each other, with a maximum difference of 3 % observed between the sine wave without crest and sine wave. But the efficiency of sine wave without crest and sin wave without trough are generally higher; For a pressure ratio of 2.5, the efficiency curves for single side clipped sine waves (sine wave without crest and sine wave without trough) are significantly higher than other two with a maximum difference of 10 %; As the pressure ratio reaches 3, the four curves separate from each other. The sine wave without trough exhibits the highest adiabatic efficiency, standing at 8 % above the sine wave and 5 % above the sine wave without crest when stroke is 8 mm. However, with the increasing stroke, the adiabatic efficiency for sine wave without crest becomes close to sine wave without trough. The adiabatic efficiency of sine wave without crest and trough is 4 % lower than the sine wave. In the test rig, the mass flow rate is almost 0 at higher pressure ratios. Thus, higher pressure ratios were not tested in this work.

According to the adiabatic efficiency shown above, the single side clipped sine waves perform better than the two others. The sine wave without trough shows the highest adiabatic efficiency in four driving voltage waveforms. At higher pressure ratio, the adiabatic efficiency appears to change more with stroke. From stroke of 8 mm to 12 mm, the adiabatic efficiency changes 2 % for the same waveform at pressure ratio of 2, while changes 20 % at pressure ratio of 3. Fig. 11shows the current, displacement and body pressure for four different driving voltage waveforms with stroke of 12 mm, pressure ratio of 3, and frequency at 31 Hz, where a to b is compression process, b to c is the discharge process, c to d is the expansion process, d to e is the suction process. The current and displacement at resonance has a 90° phase difference. For sine wave without trough, the compressor voltage is higher than others for expansion process due to voltage deforming as shown in Fig. 9. Simultaneously, the current in expansion process is also higher. This leads to a larger electromagnetic force, subsequently increasing the acceleration of the piston. As shown in Fig. 12, the acceleration of sine wave without trough also exceeds that of other waveforms in this stage, which allows the piston to reach the datum position more quickly. The faster arrival of the piston at the datum position during expansion process minimises the gas leakage from the compression chamber into the body side which makes body pressure change less compared to other 3 waveforms. As a result, the bleed flow decreases, and this leads to higher main mass flow delivered by the compression process and thus increases adiabatic efficiency. With higher pressure ratios, this influence is more significant due to increased gas leakage across the radial clearance, evidenced by Liang [28].

The compression process of the sine wave without crest has similar variation to the expansion process of the sine wave without trough. Compared with expansion process, the increasing cylinder pressure during compression process leads to more gas leakage. That makes adiabatic efficiency of the sine wave without crest lower than that of sine wave without trough.

5. Conclusions

This paper experimentally investigated the effects of driving voltage waveforms on an oil-free linear compressor. Sine wave without crest, sine wave without trough, sine wave, and sine wave without both crest and trough were tested, and their performances were evaluated. The primary conclusions are outlined as below:

(1) The single side clipped sine waves (sine wave without crest and sine wave without trough) show higher adiabatic efficiency than the sine wave and sine wave without crest and trough. This is because the former two waveforms can reduce the gas leakage across the radial clearance during compression leading to lower body pressure variation and higher mass flow rate. The sine wave without trough shows the highest adiabatic efficiency, which is 8 % higher than that of sine wave and 5 % higher than that of sine wave without crest.
(2) The mass flow rates of single side clipped sine waves are similar and both higher than that of sine wave, and the specific mass flow rate of the sine wave without trough is 10.4 % higher than that of the sine wave without crest.

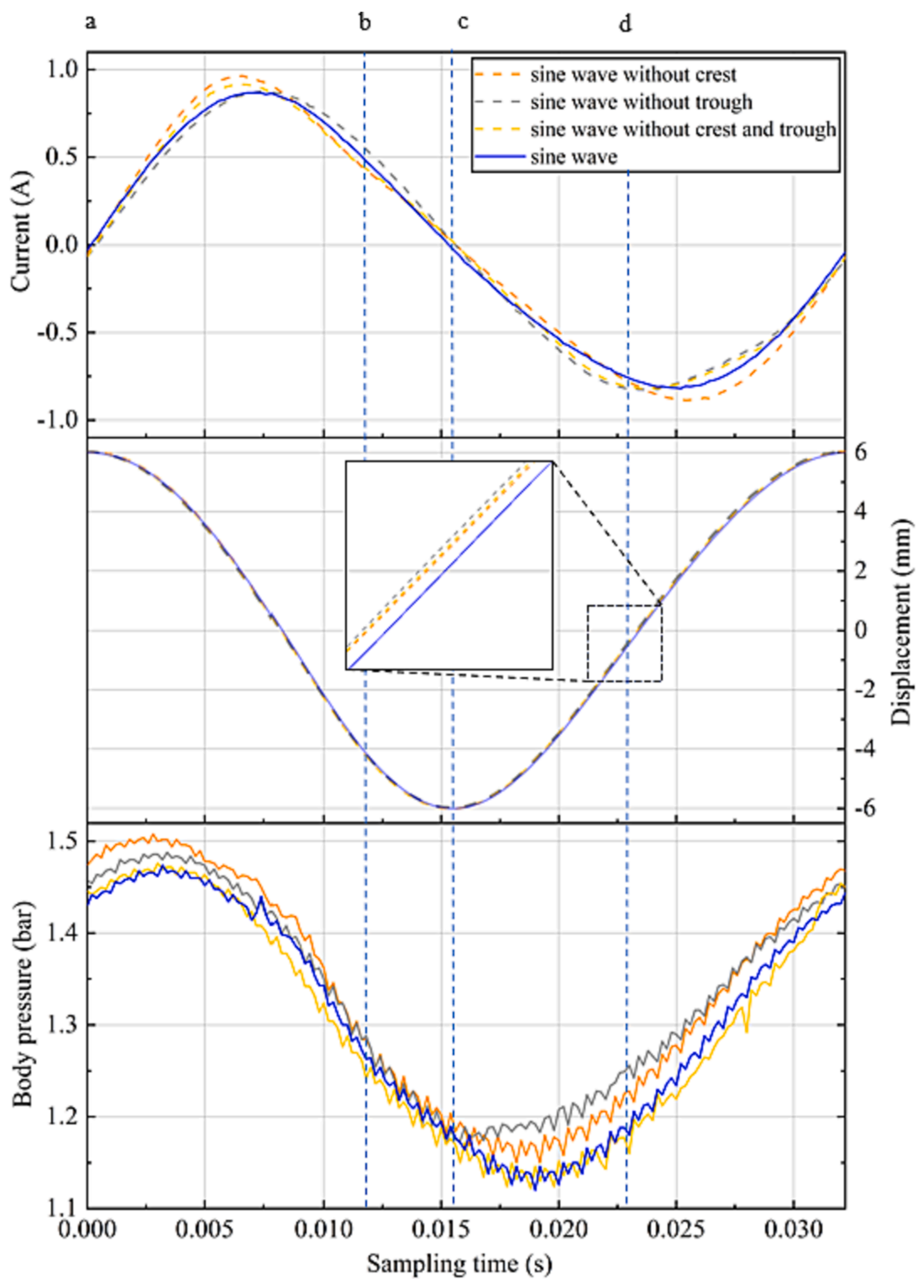

Fig. 11. Current, displacement and body pressure for four different driving voltage waveforms with stroke of 12 mm, pressure ratio of 3 and frequency of 31 Hz.

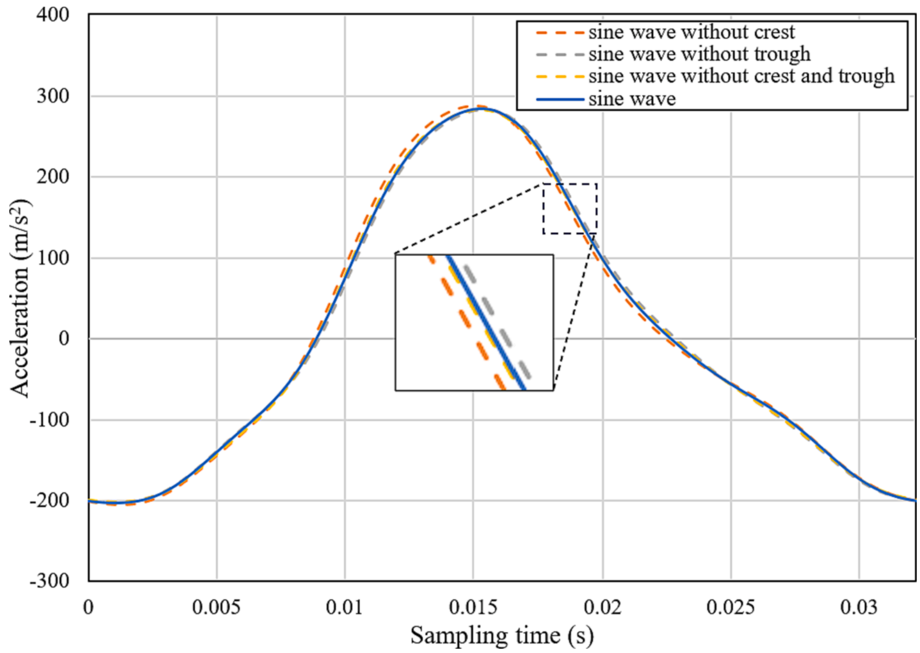

Fig. 12. Acceleration for four different driving voltage waveforms with stroke of 12 mm, pressure ratio of 3 and frequency of 31 Hz.

(3) Motor efficiencies for four waveforms are very close with 1 % difference. This is because the PID controller keeps tuning the input voltage at truncated side to achieve preset stroke for three modulated waveforms.
(4) The effect of voltage waveforms is more significant at higher pressure ratios because the gas leakage increases with pressure ratios. Future work will be looking at the effect of waveforms at higher pressure ratios.

CRediT authorship contribution statement

Nibin Qian: . **Chunhui Yang:** Investigation. **Changtong Xu:** Formal analysis. **Zhaohua Li:** Resources. **Kun Liang:** . **Zhennan Zhu:** Validation. **Xinwen Chen:** Visualization.

Declaration of competing interest

The authors declare that they have no known competing financial interests or personal relationships that could have appeared to influence the work reported in this paper.

Data availability

Data will be made available on request.

References

[1] R.G. Ross, Aerospace coolers: a 50-year quest for long-life cryogenic cooling in space, in: Cryogenic Engineering, Springer, New Yor, NY, 2007, pp. 225–284.
[2] A. Bijanzad, A. Hassan, I. Lazoglu, Analysis of solenoid based linear compressor for household refrigerator, Int. J. Refrig. 74 (2017) 116–128.
[3] H. Zou, X. Li, M. Tang, C. Tian, X. Chen, Performance analysis of linear compressor using R290 for commercial refrigerator, Int. J. Refrig 109 (2020) 55–63.
[4] N.R. Van der Walt, R. Under, The simulation and design of a high efficiency, lubricant free, linear compressor for a domestic refrigerator, 1992.
[5] Z. Zhu, K. Liang, Z. Li, H. Jiang, Z. Meng, Thermal-economic-environmental analysis on household refrigerator using a variable displacement compressor and low-GWP refrigerants, Int. J. Refrig. 123 (2021) 189–197.
[6] K. Liang, R. Stone, M. Dadd, P. Bailey, A novel linear electromagnetic-drive oil-free refrigeration compressor using R134a, Int. J. Refrig. 40 (2014) 450–459.
[7] B. Ku, J. Park, Y. Hwang, J. Lee, Performance evaluation of the energy efficiency of crank-driven compressor and linear compressor for a household refrigerator, 2010.
[8] K. Liang, A review of linear compressors for refrigeration, Int. J. Refrig. 84 (2017) 253–273.
[9] J.K. Kim, J.B. Kim, Modulation characteristics of a linear compressor for evaporating and condensing temperature variations for household refrigerators, Int. J. Refrig. 40 (2014) 370–379.
[10] Z. Li, K. Liang, H. Jiang, Thermodynamic analysis of linear compressor using R1234yf, Int. J. Refrig. (2019).
[11] C.R. Bradshaw, E.A. Groll, S.V. Garimella, Linear compressors for electronics cooling: energy recovery and its benefits, Int. J. Refrig. 36 (7) (2013) 2007–2013.
[12] K. Liang, R. Stone, W. Hancock, M. Dadd, P. Bailey, Comparison between a crank-drive reciprocating compressor and a novel oil-free linear compressor, Int. J. Refrig. 45 (2014) 25–34.
[13] P.B. Bailey, M.W. Dadd, N. Hill, C.F. Cheuk, J. Raab, E. Tward, High Performance Flight Cryocooler Compressor. Cryocoolers 11 (2002) 169–174.
[14] K. Liang, M. Dadd, P. Bailey, Clearance seal compressors with linear motor drives. Part 1: Background and system analysis, Proc. Inst. Mech. Eng. Part a: J. Power Energy 227 (3) (2013) 242–251.
[15] R. Unger, S. Novotny, A high performance linear compressor for CPU cooling, in: Proceedings of International Compressor Engineering Conference, 2002, pp. C23–C33.
[16] H. K. Lee, G.Y. Song, J.S. Park, E.P. Hong, W.H. Jung, K.B. Park, Development of the linear compressor for a household refrigerator, 2000.
[17] H. Lee, S.S. Jeong, C.W. Lee, H.K. Lee, Linear compressor for air-conditioner. Proceedings of International Compressor Engineering Conference, 2004.
[18] K. Liang, R. Stone, M. Dadd, P. Bailey, The effect of clearance control on the performance of an oil-free linear refrigeration compressor and a comparison between using a bleed flow and a DC current bias, Int. J. Refrig. 69 (2016) 407–417.
[19] X. You, L. Qiu, X. Zhi, X. Tao, J. Wang, Study on the method of improving the input power of the linear compressor in a high capacity pulse tube cryocooler, Int. J. Refrig. 96 (2018) 139–146.
[20] H. Jiang, Z. Li, K. Liang, Performance of a linear refrigeration compressor with small clearance volume, Int. J. Refrig. 109 (2020) 105–113.
[21] Z. Zhu, K. Liang, Z. Li, H. Chen, A novel resonant frequency tracking technique for linear compressors, Mech. Syst. Sig. Process. 201 (2023) 110675.
[22] J. Tan, H. Dang, Effects of the driving voltage waveform on the performance of the Stirling-type pulse tube cryocooler driven by the moving-coil linear compressor, Int. J. Refrig. 75 (2017) 239–249.
[23] C. Li, J. Li, L. Tang, J. Sun, H. Zou, J. Cai, Effects of the driving voltage waveform on the performance of vapor compression cycle system driven by the moving coil oil-free linear compressor, Int. J. Refrig. 108 (2019) 200–208.
[24] Y. Wei, Z. Zuo, B. Jia, H. Feng, K. Liang, Influence of piston displacement profiles on the performance of a novel dual piston linear compressor, Int. J. Refrig. 117 (2020) 71–80.
[25] E. Silva, T. Dutra, Piston trajectory optimization of a reciprocating compressor, Int. J. Refrig 121 (2021) 159–167.
[26] K. Liang, A novel linear electromagnetic-drive oil-free refrigeration compressor, University of Oxford, 2014. Doctoral dissertation.
[27] K. Ueno, R.E. Bye, K.S. Hunter, Compressor Efficiency Definitions, VAIREX Corporation and University of Colorado, 2003.
[28] K. Liang, Analysis of oil-free linear compressor operated at high pressure ratios for household refrigeration, Energy 151 (2018) 324–331.